

# Monolithic Millimeter Wave Optical Receivers

Jinwook Burm, Kerry I. Litvin, Glenn H. Martin, *Member, IEEE*,  
 William J. Schaff, *Member, IEEE*, and Lester F. Eastman, *Life Fellow, IEEE*

**Abstract**—A single stage monolithic millimeter wave optical receiver circuit was designed and fabricated using a metal-semiconductor-metal (MSM) photodetector and a pSemidomorphic Modulation Doped Field Effect Transistors (SMODFET) on a GaAs substrate for possible applications in chip-to-chip and free space communications. The MSM photodetector and the SMODFET epitaxial material were grown by molecular beam epitaxy (MBE). Device isolation was achieved using an epitaxially grown buffer between the MSM detector layers and SMODFET. The photodetector was designed for maximum absorption at optical wavelength of 770 nm light and the SMODFET impedance matching network was optimized for 44 GHz. The monolithic millimeter wave optical receiver circuit achieved 3 dB gain over a photodetector at 39 GHz, which was the limit of the measurement system. TOUCHSTONE model of the circuit indicated 6.6 dB gain over the photodetector and 5.7 dB total gain including the insertion loss of the photodetector at 44 GHz.

## I. INTRODUCTION

**P**HOTODETECTORS are an essential component in optoelectronic integrated circuits. The demands for fast and sensitive photodetectors have driven a great deal of research work in this area resulting many improvements over the years. Metal-semiconductor-metal (MSM) photodetectors are preferred over p-i-n photodetectors in optoelectronic circuits due to their planar structure (easily integrated monolithically) and relatively simple design in combination with outstanding frequency performance [1], [2]. MSM photodetectors have been demonstrated with 3 dB bandwidth of greater than 350 GHz [3], [4].

Recent developments for achieving ultrafast MSM photodetectors have been in decreasing the gap between the fingers for short carrier transit time, and decreasing the capacitance by reducing the overall size. In real applications, the sensitivity is an important parameter to be considered and is difficult to optimize for MSM photodetectors. The low sensitivity of MSM photodetectors is due in part to the metal finger shadowing. Additional sensitivity degradation occurs for the MSM photodetectors on GaAs due to the electron-hole pair recombination at the exposed GaAs surface and the approximately 30% reflection at the GaAs-air junction. These

Manuscript received April 7, 1995; revised July 22, 1996. This work was supported by Rome Laboratory under Contract F30602-91-C-0063 and by Hughes Research Laboratory. This work was performed in part at the Cornell Nanofabrication Facility (a member of the National Nanofabrication Users Network) which is supported by the National Science Foundation under Grant ECS-9319005. Cornell University, and industrial affiliates.

J. Burm, G. H. Martin, W. J. Schaff, and L. F. Eastman are with the School of Electrical Engineering and Cornell Nanofabrication Facility, Cornell University, Ithaca, NY USA.

K. I. Litvin is with the Missile and Space Section, Lockheed Martin, King of Prussia, PA USA.

Publisher Item Identifier S 0018-9480(96)07912-4.

effects in combination with the possible absorbing surface area covered by the metal electrodes can reduce the overall quantum efficiency a great deal. To increase the sensitivity of the MSM photodetectors without decreasing the speed, we employed an AlGaAs cap layer, to minimize the surface recombination of the optically created carriers. The cap layer also reduces the reflectance of the top surface of the detectors. A thin GaAs absorption layer is employed to decrease the carrier transit time. Buried Bragg reflector layers are used to reflect unabsorbed light back into the absorption layer [5], [6]. The idea of employing Bragg reflector layers has previously been introduced for Schottky photodiodes [7], phototransistors [8], and p-i-n detectors [9].

Millimeterwave optical receivers have been fabricated monolithically integrating an MSM photodetectors and a transistor for possible applications in chip-to-chip communications as well as free space communications. The optical receiver layers were designed for the maximum absorption of 770 nm light signals. For amplification transistors, pSemidomorphic Modulation Doped Field Effect Transistors (SMODFET's) were used. Coplanar waveguide (CPW) transmission line matching networks connected the detectors and SMODFET's. The optical receiver circuits were designed for a narrow bandwidth about 44 GHz.

## II. LAYER STRUCTURE

To increase the sensitivity of MSM photodetectors, the layer structure was carefully designed for the maximum light absorption. By following the method of layer design for the maximum absorption of the incident light as described at [2], [6], the layer structures were determined for the best absorption of the light at 770 nm. The 770 nm light can be easily obtained from Ti-Sapphire lasers. The optical detector structure includes 16.5 pairs of Bragg reflector layers, 3120 Å GaAs absorption layer, and 1906 Å Al<sub>0.3</sub>Ga<sub>0.7</sub>As cap layer. The thickness of the cap layer was thicker than the calculated optimum thickness (1106 Å), where the absorption was maximum, to allow for process tolerances. The Al mole fractions in the cap layer and in the quarter wavelength Bragg reflector sections were chosen so that these layers were nonabsorbing at the wavelengths of interest (Fig. 1). The GaAs absorption layer was the only absorbing layer. The Al<sub>0.3</sub>Ga<sub>0.7</sub>As cap layer is important in two aspects. First, by having an Al<sub>0.3</sub>Ga<sub>0.7</sub>As cap layer on the top of the GaAs absorption layer, the recombination velocity toward the surface, or heterojunction, is sharply reduced by removing recombination centers on exposed GaAs [6]. Second, by adjusting the thickness of the Al<sub>0.3</sub>Ga<sub>0.7</sub>As cap layer, the

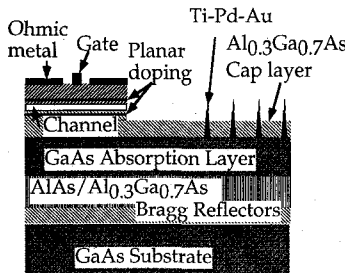


Fig. 1. Cross section of the optical receiver layer. The SMODFET layer on the top of the photodetector layer utilizes strained  $In_{0.2}Ga_{0.8}As$  channel.

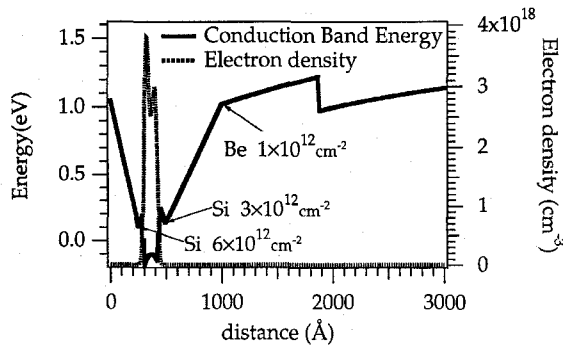


Fig. 2. The conduction band plot as a function of the distance from the gate.

377  $\Omega$  characteristic impedance of the air can be matched to the optical resonant impedance of the photodetector structure. The impedance matching reduces the reflectance to nearly negligible levels [2] and [6].

The photodetector layers were followed by the double-doped SMODFET layers. The SMODFET layers were composed of a  $1 \times 10^{12} \text{ cm}^{-2}$  planar p-doped layer, 500 Å  $Al_{0.3}Ga_{0.7}As$  layer,  $3 \times 10^{12} \text{ cm}^{-2}$  planar n-doped layer, 50 Å  $Al_{0.3}Ga_{0.7}As$  spacer, 120 Å  $In_{0.2}Ga_{0.8}As$  channel sandwiched between two 20 Å GaAs layers, 30 Å  $Al_{0.3}Ga_{0.7}As$  spacer,  $6 \times 10^{12} \text{ cm}^{-2}$  planar n-doped layer, 250 Å  $Al_{0.3}Ga_{0.7}As$  barrier and 400 Å n-doped GaAs cap layer for metal contacts. The planar p-doped layer was employed to tightly confine the 2-DEG in the pseudomorphic  $In_{0.2}Ga_{0.8}As$  channel. The energy band diagram of the SMODFET layer can be calculated by solving the Schrödinger equation and the Poisson equation simultaneously. Using a computer program called CBAND [10], we obtained the energy band diagram as shown at Fig. 2. The whole optical receiver layers were grown using Varian Gen II molecular beam epitaxy (MBE). Be and Si were used for p and n doping, respectively.

### III. PSEUDOMORPHIC MODULATION DOPED FIELD EFFECT TRANSISTORS

The transistors were fabricated using standard processing procedures—mesa isolation, ohmic metal, and gate metal deposition. For mesa isolation, the citric acid solution [citric acid (0.2 M) :  $H_2O_2 = 50:1$ ] was used. The etch rate was  $\sim 6 \text{ \AA/s}$ . During the mesa isolation, a part of the photodetector cap layer was etched away. As mentioned earlier, a certain thickness of the cap layer was required to match the characteristic impedance of the photodetector layer to that of

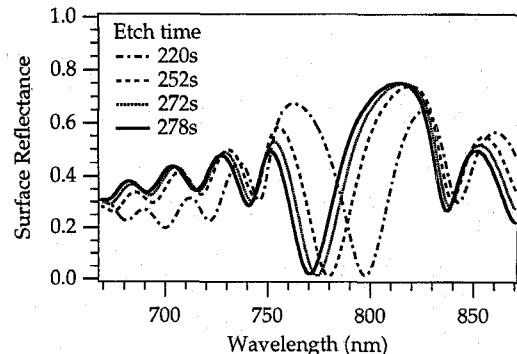


Fig. 3. Measured surface reflectance of the optical receiver layer. The reflectance curves measured after the specified etch time.

the air. Thus the surface reflectance was monitored closely in order to stop at the right place for the minimum reflection from the surface at the desired wavelength. The minimum reflection is important as it implies maximum absorption of incident light. A spectrophotometer, Cary 5 by Varian, was used for the surface reflectance measurement. As the etch proceeded, the wavelength of the minimum reflectance shifted, allowing us to stop at the right wavelength where we wanted to tune the photodetector layer. Fig. 3 shows how the measured surface reflectance changed as the depth of etch varies. Ni/AuGe/Ag/Au were used for ohmic contacts. After the ohmic metal deposition, samples were annealed at 450°C for 10 s. A transfer length model (TLM) pattern showed a contact resistance of  $0.1 \Omega \cdot \text{mm}$ . Ti/Pd/Au gate metals were deposited after the electron-beam lithography and recess etch with citric acid. The gate width was 75  $\mu\text{m}$  and the gate length was about 0.15  $\mu\text{m}$ . The fabricated transistors showed a cut-off frequency,  $f_T$ , of 90 GHz and maximum oscillation frequency,  $f_{\max}$ , of 100 GHz, however, some variations in device performance were observed.

### IV. PHOTODETECTORS

Circular-aperture MSM photodetectors were employed in the optical receiver circuits (Fig. 4). Having no extra area, the circular-aperture photodetectors show advantages over square or rectangular-aperture devices with the same detection area because of their smaller capacitance [11]. 150 Å Ti, 150 Å Pd, and 600 Å Au were used for finger metallization. Before the evaporation of metal fingers, 90% of AlGaAs cap layer had been etched using citric acid as described above. A stylus profile was used to monitor the etch depth. Ti was used for a good Schottky barrier. Pd was used for a diffusion barrier between Ti and Au. Au was used for a good electrical contact. In general, the quantum efficiency of MSM photodetectors is difficult to determine due to low frequency gain mechanisms (more than 100% of quantum efficiency) [12], [13]. The internal quantum efficiency of gain-suppressed photodetectors was measured for detectors fabricated on about the same layer structure but for different wavelength. The internal efficiency was 82% at 5 V bias and 94% at 10 V bias with 54.4  $\mu\text{W}$  optical power [6]. No careful quantum efficiency measurement was done for the detectors on the wafer due to the low frequency gain, but 0.1 A/W (3% of quantum efficiency) of

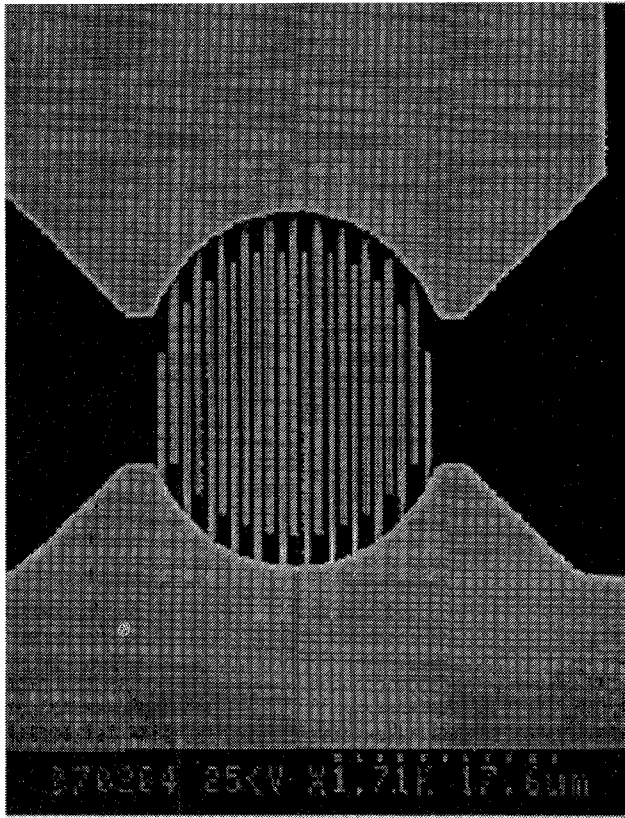


Fig. 4. A circular MSM photodetector in a circuit. The finger width and the gap between the fingers are  $0.5\text{ }\mu\text{m}$ .

responsivity was obtained for  $0.5\text{ }\mu\text{m}$  gap and  $0.5\text{ }\mu\text{m}$  finger width MSM photodetectors at  $10\text{ mW}$  of optical power. The low quantum efficiency was attributed to excessive carrier recombinations from the high optical power.

##### V. BIAS LINES AND BIAS ISOLATIONS

Coplanar wave guide (CPW) transmission lines were employed for matching and filtering networks. For dc bias, capacitor-isolated dc bias lines and ground plane capacitor dc isolation were used. The capacitor-isolated dc bias lines [Fig. 5(a)] consisted of a metal strip used as a dc conductor with a connecting resistor between the bias line and the CPW line. The ground plane of the CPW ran over the metal strip with dielectric isolation in between, forming a capacitor. Thus the metal strip running under the ground plane will be an RF-short due to the capacitor. The desired bias is achieved with a resistor. The resistor, used to connect the end of the bias line and the CPW lines, should be high enough not to interrupt the signal flow too much. Epitaxial resistors with  $600\text{--}700\text{ }\Omega$  were utilized on  $50\text{ }\Omega$  transmission lines.

For dc bias isolation [Fig. 5(b)], ground plane capacitor isolation [14], [15] was employed. The ground plane capacitor isolation had overlay capacitors in ground planes, so that each section of the ground planes can be biased separately. Each capacitor was  $20 \times 300\text{ }\mu\text{m}^2$  and had about  $3\text{ pF}$  of capacitance based on previous measurements.

A GaAs substrate was used to fabricate the test patterns [Fig. 5(a) and (b)]. For CPW line metallization,  $300\text{ \AA}$  of Ti,

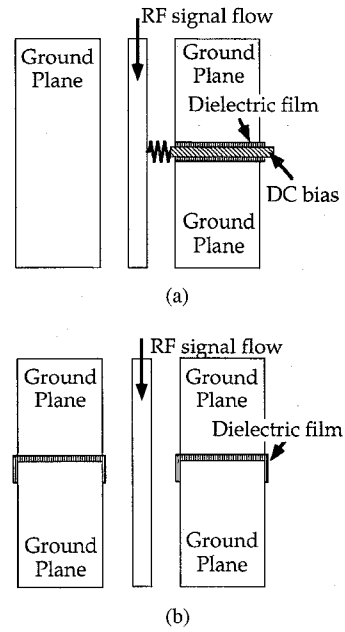


Fig. 5. Bias line and bias isolation test patterns and measured insertion loss.  $1000\text{ }\mu\text{m}$  long  $50\text{ }\Omega$  CPW transmission lines were used. (a) The schematics of capacitor-isolated bias lines of which insertion loss was  $-0.26\text{ dB}$  at  $44\text{ GHz}$  and (b) the schematics of ground plane capacitor isolation of which insertion loss was  $-0.18\text{ dB}$  at  $44\text{ GHz}$ .

$200\text{ \AA}$  of Pd, and  $5500\text{ \AA}$  of Au were used. The capacitors in the test structures were composed of  $1000\text{ \AA}$  of metal ( $150\text{ \AA}$  of Ti,  $50\text{ \AA}$  of Pd, and  $800\text{ \AA}$  of Au),  $1000\text{ \AA}$  of E-beam evaporated  $\text{SiO}_2$  and  $6000\text{ \AA}$  of overlay metal, of the same composition as the CPW lines. The main CPW line fabricated was  $1000\text{ }\mu\text{m}$  long and had a  $50\text{ }\Omega$  characteristic impedance with the following dimensions,  $50\text{ }\mu\text{m}$  wide center conductor and  $35\text{ }\mu\text{m}$  gaps between the center conductor and the ground planes. The characteristic impedances were calculated using a commercially available CAD program. The measured insertion loss was  $-0.26\text{ dB}$  for the capacitor isolated bias lines and  $-0.18\text{ dB}$  for the ground plane capacitor isolation at  $44\text{ GHz}$ .

##### VI. OPTICAL RECEIVER DESIGN AND FABRICATIONS

For the fabrication of the single stage optical receiver circuits, SMODFET's and photodetectors were fabricated and their S-parameters were measured up to  $50\text{ GHz}$  using an HP8510C network analyzer. Based on the measured S-parameter values at  $44\text{ GHz}$  and assuming unilateral conditions ( $S_{21} \approx 0$ ), we conjugately matched the S-parameters of adjacent elements [16], for example,  $S_{11}^*$  of photodetectors and  $S_{11}$  of transistors, by way of  $50\text{ }\Omega$  CPW transmission lines and one or two quarter wavelength impedance transformers. The  $S_{22}$  of the transistor was matched to  $50\text{ }\Omega$ . Two quarter wavelength impedance transformers were used instead of one, if the impedance of a single impedance transformer was either too small or too large to be able to fabricate without significant loss of signal power. In case of CPW transmission lines fabricated on GaAs, the usable impedance value varies approximately from  $19\text{--}110\text{ }\Omega$ . If an impedance value is out of this range, either capacitive loss and resistive loss of the transmission line increases sharply. After the impedance

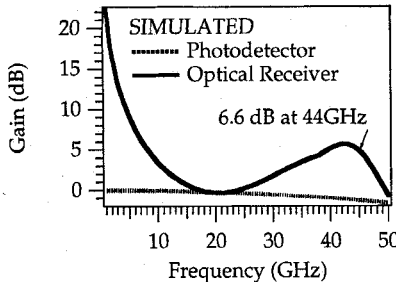


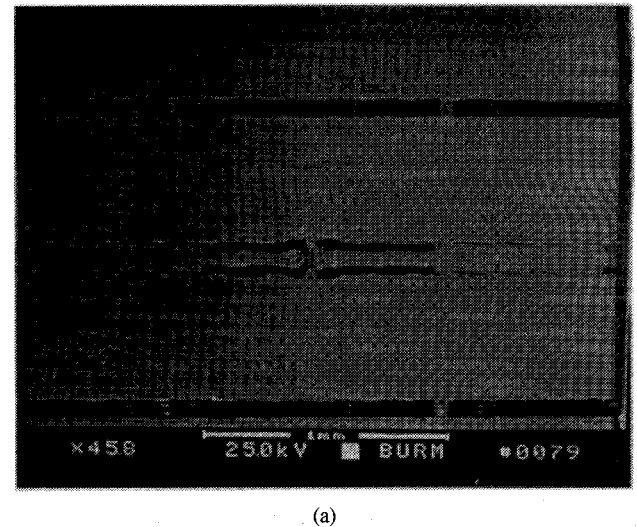
Fig. 6. A simulated gain of single stage receiver circuit. The amplifier showed 6.6 dB gain over the photodetector at 44 GHz. The total gain including the insertion loss of the photodetector was 5.7 dB at 44 GHz.

matching procedure, a CAD program [17] was used to predict the circuit response. For this purpose, the frequency response of photodetectors was modeled from both intrinsic carrier response [18] and extrinsic circuit response as described in [2]. For SMODFET's, the measured values were used. The simulated gain of a single stage receiver circuit was 6.6 dB over the photodetector at 44 GHz. The total gain including the insertion loss of the photodetector was 5.7 dB at 44 GHz (Fig. 6).

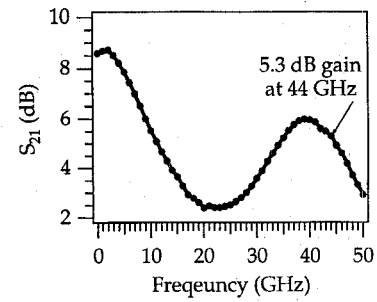
The actual fabrication processes of the optical receiver circuits began with the mesa isolation and ohmic level of transistors. However, the gate level of the transistors was done at the end of the fabrication process, to avoid any possible damage to the delicate narrow gates. After the mesa etch and ohmic contacts to the transistors, the metal fingers of photodetectors, the bottom metal and the  $\text{SiO}_2$  film of capacitors, and the ground plane of CPW were fabricated.

Single stage amplifiers composed of a transistor and associated matching networks, but without photodetectors, were also fabricated [Fig. 7(a)]. A quarter wavelength transformer and a  $50 \Omega$  transmission line were used to match either  $S_{11}$  or  $S_{22}$  of the transistors to  $50 \Omega$ . The amplifiers were easier to measure than the optical receiver circuits at 44 GHz. The single stage amplifiers provided with useful information on how well the matching at 44 GHz worked. The measured result showed 5.3 dB gain at 44 GHz [Fig. 7(b)]. However the maximum gain occurred at 40 GHz instead of at 44 GHz where the circuit was designed, from a slight mismatch of the circuit. This was largely due to the process variations of the transistors.

Optical receiver circuits (Fig. 8) were also fabricated and tested. Two beating Ti-Sapphire lasers at 770 nm were used for these measurements. The beating frequency could be measured using a fabricated photodetector and a Tektronics 2782 spectrum analyzer. The beating signal was fed into a single mode optical fiber to a photodetector. The optical power measured was 10 mW at the end of the fiber. As a way to observe the amplification after the photodetectors, we measured a single detector without any amplifying section first, then measured an optical receiver circuit. When the beating laser beam was moved to another photodetector, we maximized the photo-current and made sure that the photocurrent from the photodetector was about the same as before. The beating frequency of the two laser beams was set to 39 GHz. We measured the RF signal for two minutes, registering all the new maximum peaks for a more reliable



(a)



(b)

Fig. 7. (a) Fabricated single stage amplifier without a photodetector and (b) the measured results with 5.3 dB gain at 44 GHz.

comparison. The resolution bandwidth and sweep time of the spectrum analyzer were 300 kHz and 130 ms, respectively. A needle probe was used to monitor the gate bias for the initial bias settings, making a contact on the center conductor of the CPW near the gate of the SMODFET's. The measured RF results with the needle probe engaged show little difference with the needle probe up in the air at high frequency ( $>20$  GHz), suggesting a good RF blocking of the needle probe in the frequency range. Thus the needle probe was placed during the RF measurements for a careful gate bias monitor. The signal from a single photodetector was  $-40$  dBm, while that from an optical receiver circuit measured right after the single photodetector was  $-37$  dBm indicating about 3 dB gain at 39 GHz. We could not test the optical receiver circuits at 44 GHz, where the circuits were designed to work, due to the limitation of the spectrum analyzer. The results of the single stage amplifier at 44 GHz and the  $\sim 3$  dB gain of the postdetection amplifier of the optical receiver circuit at 39 GHz are favorable to expect a working result of optical receiver circuits at 44 GHz.

## VII. CONCLUSION

Monolithic integrated photodetectors and transistors were incorporated into optical receiver circuits tuned to 44 GHz. The devices were fabricated on GaAs based MBE grown layers. The photodetector layers were optimized to have high quantum

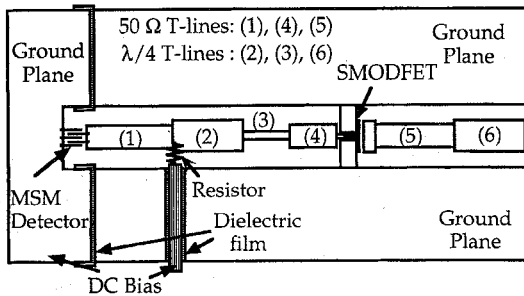


Fig. 8. Schematics of fabricated optical receiver circuits [19].

efficiency and high speed for 770 nm optical wavelength. A double-doped InGaAs channel SMODFET's layer structure was used for the post-detection amplifiers. CPW transmission lines were used for the matching and filtering networks. After fabricating individual circuit elements, their *S*-parameters were measured. The *S*-parameters of the photodetectors and transistors were used to design optical receiver circuits. To apply dc bias, capacitor isolated bias lines, showing  $-0.26$  dB insertion loss at 44 GHz with  $1000 \mu\text{m}$  transmission line, were employed. For bias isolation, ground plane capacitor isolation, with  $-0.18$  dB insertion loss at 44 GHz, were used. The fabricated single stage amplifier without a photodetector was measured up to 50 GHz with an HP8510C network analyzer, showing 5.3 dB gain at the design frequency. Two beating Ti-Sapphire lasers and a 40 GHz spectrum analyzer were used to measure the optical receiver circuit. The measured result at 39 GHz showed about 3 dB gain over the photodetectors. However the optical receiver could not be measured at 44 GHz due to an instrumental limit of 40 GHz.

#### ACKNOWLEDGMENT

The authors would like to thank M. Jaspan and A. Davidson for the preparation of lasers, N. Koliias and M. Vaughn for the use of a network and spectrum analyzers, and Prof. R. C. Compton for valuable ideas and suggestions.

#### REFERENCES

- [1] M. Ito, O. Wada, K. Nakai, and T. Sakurai, "Monolithic integration of a metal-semiconductor-metal photodiode and a GaAs preamplifier," *IEEE Electron Device Lett.*, vol. EDL-5, pp. 531-532, 1984.
- [2] K. Litvin, J. Burm, D. Woodard, W. Schaff, and L. F. Eastman, "High speed optical detectors for monolithic millimeter wave integrated circuits," in *IEEE MTT-S Dig.*, vol. 2, 1993, pp. 1063-1066.
- [3] Y. Chen, S. Williamson, T. Brock, F. W. Smith, and A. R. Calawa, "375-GHz-bandwidth photoconductive detector," *Appl. Phys. Lett.*, vol. 59, pp. 1984-1986, 1991.
- [4] S. Y. Chou and M. Y. Liu, "Nanoscale tera-hertz metal-semiconductor-metal photodetectors," *IEEE J. Quantum Electron.*, vol. 28, pp. 2358-2368, 1992.
- [5] K. I. Litvin, J. Burm, D. W. Woodard, P. Mandeville, W. J. Schaff, M. M. Gitin, and L. F. Eastman, "High-speed MSM photodetectors for millimeter waves," in *SPIE—Optoelectronic Sig. Proc. Phased Array Antennas III*, Proc. SPIE—Int. Soc. Opt. Eng., Orlando, FL, 1992, vol. 1703, pp. 313-320.
- [6] J. Burm, K. I. Litvin, D. W. Woodard, W. J. Schaff, P. Mandeville, M. A. Jaspan, M. M. Gitin, and L. F. Eastman, "High-frequency, high-efficiency MSM photodetectors," *IEEE J. Quantum Electron.*, vol. 31, pp. 1504-1509, 1995.
- [7] A. Chin and T. Y. Chang, "Multilayer reflectors by molecular-beam epitaxy for resonance enhanced absorption in thin high-speed detectors," *J. Vac. Sci. Tech. B*, vol. 8, pp. 339-342, 1990.
- [8] M. S. Ünlü, K. Kishino, J.-I. Chyi, L. Arsenault, J. Reed, S. N. Mohammad, and H. Morkoç, "Resonant cavity enhanced AlGaAs/GaAs heterojunction phototransistors with an intermediate InGaAs layer in the collector," *Appl. Phys. Lett.*, vol. 57, pp. 750-752, 1990.
- [9] I.-H. Tan, J. J. Dudley, D. I. Babic, D. A. Cohen, B. D. Young, E. L. Hu, J. E. Bower, B. I. Miller, U. Koren, and M. G. Young, "High quantum efficiency and narrow absorption bandwidth of the wafer-fused resonant  $\text{In}_{0.53}\text{Ga}_{0.47}\text{As}$  photodetectors," *IEEE Photonics Tech. Lett.*, vol. 6, no. 7, pp. 811-813, 1994.
- [10] M. Foisy, "A physical model for bias dependence of the modulation-doped field-effect transistor's high frequency performance," Ph.D. dissertation, Cornell University, 1990.
- [11] J. Burm, K. I. Litvin, W. J. Schaff, and L. F. Eastman, "Optimization of high-speed metal-semiconductor-metal photodetectors," *IEEE Photon. Tech. Lett.*, vol. 6, pp. 722-724, 1994.
- [12] J. Burm and L. F. Eastman, "Low-frequency gain in MSM photodiodes due to charge accumulation and image force lowering," *IEEE Photon. Tech. Lett.*, vol. 8, pp. 113-115, 1996.
- [13] M. Klingenstein, J. Kuhl, J. Rosenzweig, C. Moglestue, A. Hülsmann, J. Schneider, and K. Köhler, "Photocurrent gain mechanisms in metal-semiconductor-metal photodetectors," *Solid-State Electron.*, vol. 37, no. 2, pp. 333-340, 1994.
- [14] R. C. Compton, private communication.
- [15] K. C. Gupta, *Microstrip Lines and Slotlines*. Dedham, MA: Artech House, 1979, ch. 7.
- [16] D. M. Pozar, *Microwave Engineering*. Reading, MA: Addison-Wesley, 1990, p. 99.
- [17] Touchstone®, EEsof Inc., 5601 Lindero Canyon Rd., Westlake Village, CA 91362-4020.
- [18] J. B. D. Soole and H. Schumacher, "Transit-time limited frequency response of InGaAs MSM photodetectors," *IEEE Trans. Electron Devices*, vol. 37, pp. 2285-2290, 1990.
- [19] J. Burm, K. I. Litvin, G. H. Martin, W. J. Schaff, and L. F. Eastman, "Monolithic millimeter wave optical receivers using MSM photodetectors and SMODFET's," in *Proc. 22nd Int. Symp. Comp. Semiconductors*, Cheju Island, Korea, 1995.

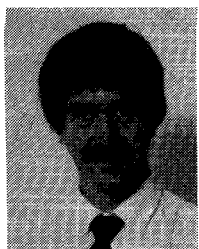
**Jinwook Burm** was born in Korea in 1964. He received the B.S. degree in physics from Seoul National University, Seoul, Korea, in 1987, the M.S. degree in physics from the University of Michigan, Ann Arbor, in 1989, and the Ph.D. degree in applied physics from Cornell University, Ithaca, NY, in 1995. After the Ph.D., he stayed at Cornell University for postdoctoral work.

Since September, 1996 he has been with Lucent Technology Bell Labs in Murray Hill, NJ. His research interests include the growth and characterization of compound semiconductor devices including III-nitrides.

**Kerry I. Litvin** was born in Philadelphia, PA, 1962. He received the B.S. degree with high honors from Drexel University, Philadelphia, in 1985, the M.S. degree from the California Institute of Technology in 1986, and the Ph.D. degree from Cornell University, Ithaca, NY, in 1994, all in electrical engineering.

He spent several semesters working as a Member of the Technical Staff at the Hughes Research Laboratories in Malibu, CA. He is currently with Lockheed Martin missile and space section in King of Prussia, PA.

Dr. Litvin During his study at Cornell, he received an Amoco Oil Company Fellowship and a Hughes Aircraft Company Ph.D. Fellowship. In 1989, he also received a fellowship award from the IEEE Microwave Theory and Techniques Society. He is a member of the Eta Kappa Nu and Tau Beta Pi honor societies and is a member of the IEEE Microwave Theory and Techniques Society and the Electron Device Society. He is also affiliated with the American Physical Society.

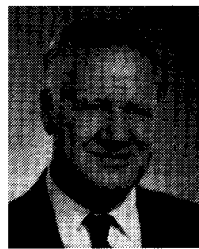


**Glenn H. Martin** (S'84-M'85) received the B.S.E.E. and M.S.E.E. degrees from the University of New Mexico, Albuquerque, NM, in 1982 and 1985, respectively.

He worked at Sandia National Labs from 1983 to 1985 in the RAD-HARD CMOS group, modeling 1 micron MOSFET's. From 1986 to 1993, he was with the RF Laboratory at Boeing's High Technology Center in Seattle, WA, where he worked on modeling on-wafer high speed III-V semiconductors for use in millimeter wave systems, in which he was the first to do on-wafer 50 GHz measurements in 1988. In 1993, he joined Prof. Eastman's research group at Cornell University, Ithaca, NY, as a graduate student working on the Ph.D. degree in electrical engineering, where his research is in PHEMT's on Indium Phosphide substrates. He is a member of Eta Kappa Nu and Tau Beta Pi.

**William J. Schaff** (S'77-M'78) graduated from Cornell University, Ithaca, NY, in 1978 in electrical engineering.

From 1978 to 1979, he was an Engineer with Harris Corporation, RF Communications Division. In January 1984, he joined the staff at Cornell where he is now a Senior Research Associate. His areas of interest are MBE growth and characterization of compound semiconductors for microwave and optical device applications, and in the epitaxial growth and electron transport properties of III-nitrides.



**Lester F. Eastman** (A'53-M'58-SM'65-F'69-LF'94) was born in Utica, NY, and received the B.S. degree in 1953, the M.S. degree in 1955, and the Ph.D. degree in 1957, all at Cornell University, Ithaca, NY.

He joined the faculty of Electrical Engineering at Cornell in 1957, and also serves as a Member of the graduate field of applied physics. Since 1965, he has been doing research on compound semiconductor materials and high speed devices and circuits, and has been active in organizing workshops and conferences on these subjects elsewhere since 1965 and at Cornell from 1967. In 1977, he joined other Cornell faculty members in obtaining funding and founding the National Research and Resource Facility for Submicron Structures at Cornell (now National Nanofabrication Facility). Also, in 1977, he founded the Joint Services Electronics Program and directed it until 1987. He has recently joined with others at Cornell to develop a large effort in high frequency/high speed optoelectronics. He has supervised more than 97 Ph.D. dissertations, more than 50 M.S. theses, and more than 50 post-doctoral studies. In his research group, effort is underway on molecular beam epitaxy, microwave transistors, high speed semiconductor lasers, high frequency photo-receivers, and fundamental phenomena in compound semiconductor quantum electron and optical devices. During the 1978 to 1979 year he was on leave at MIT's Lincoln Laboratory, and during the 1985 to 1986 year he was at IBM Watson Research Laboratory. During 1983, he was the IEEE Electron Device Society National Lecturer.

Dr. Eastman was a member of the U.S. Government Advisory Group on Electron Devices from 1978 to 1988, and has served as a consultant for several industries. From 1987 to 1993, he served as a member of the Kuratorium (Visiting Senior Advisory Board) of the Fraunhofer Applied Physics Institute in Freiburg, Germany. He was a founder in 1985 and has served as chairman of the board of directors of Northeast Semiconductors, Inc. from 1985 to 1993. He has been a Fellow of IEEE since 1969, a member of the National Academy of Engineering since 1986, and has been appointed the John L. Given Foundation Chair Professor of Engineering at Cornell in January 1985. In September 1991, he was awarded the GaAs Symposium Award, and the Heinrich Welker medal, for his "contributions to the development of ballistic electron devices, planar doping, buffer layers, and AlInAs/GaInAs/InP heterostructures." He was awarded the Alexander von Humboldt Senior Fellowship in 1994 and Aldert van der Ziel Award in 1995.